Analyses of cladding modes in photonic crystal fiber

Hyun Chul Park[*], In Kag Hwang[2], Dong Il Yeom[3], and Byoung Yoon Kim

Department of Physics, Korea Advanced Institute of Science and Technology
373-1 Guseong-dong, Yuseong-gu, Daejeon, 305-701, Korea
[2]Department of Physics, Chonnam National University
300 Yongbong-dong, Buk-gu, Gwangju 500-757, Korea
[3]4ARC Centre for Ultrahigh-bandwidth Devices for Optical Systems (CUDOS),
School of Physics, University of Sydney, NSW 2006, Australia
* wasteland@kaist.ac.kr;http://fiber.kaist.ac.kr

Abstract: Characteristics of cladding modes in a photonic crystal fiber (PCF) are numerically analyzed using the plane wave expansion method. The presence of the outer silica ring in the PCF tends to push the optical fields of the cladding modes toward the rim of the PCF, which creates 'ring modes' whose fields are tightly confined in the outer ring. The dispersion of the cladding modes are determined mainly by the dispersive property of the holey cladding structure. The optical field patterns of the cladding modes and the beatlengths between the fundamental mode and the cladding modes are also investigated.

OCIS codes: (060.5295) Photonic crystal fibers; (230.2285) Fiber devices.

References and links

1. T. A. Birks, J. C. Knight, and P. St. J. Russell, "Endlessly single-mode photonic crystal fiber," Opt. Lett. **22**, 961-963 (1997).
2. J. C. Knight, T. A. Birks, A. Ortigosa-Branch, W. J. Wadsworth, and P. St. J. Russell, "Anomalous dispersion in photonic crystal fiber," IEEE Photon. Technol. Lett. **12**, 807-809 (2000).
3. K. Suzuki, H. Kubota, M. Tanaka, M. Fujita, and S. Kawanishi, "Optical properties of a low-loss polarization-maintaining photonic crystal fibers," Opt. Express **9**, 676-680 (2001).
4. G. Kakarantzas, T. A. Birks, and P. S. J. Russell, "Structural long-period gratings in photonic crystal fibers," Opt. Lett. **27**, 1013-1015 (2002).
5. A. Diez, T. A. Birks, W. H. Reeves, B. J. Mangan, and P. S. J. Russell, "Excitation of cladding modes in photonic crystal fibers by flexural acoustic waves," Opt. Lett. **25**, 1499-1501 (2000).
6. H. S. Kim, S. H. Yun, H. K. Kim, N. Park, and B. Y. Kim, "Actively gain-flattened erbium-doped fiber amplifier over 35 nm by using all fiber acoustooptic tunable filters," IEEE Photon. Technol. Lett. **10**, 790-792 (1998).
7. S. H. Lee, K. Y. Song, and B. Y. Kim, "Fused bitapered single-mode fiber directional coupler for core and cladding mode coupling," IEEE Photon. Technol. Lett. **17**, 2631-2633 (2005).
8. S. G. Johnson and J. D. Joannopoulos, "Block-iterative frequency-domain methods for Maxwell's equations in a planewave basis," Opt. Express **8**, 173-190 (2001).
9. J. D. Joannopoulos, R. D. Meade, and J. N. Winn, *Photonic crystals* (Princeton University Press, 1995).
10. I. K. Hwang, Y. J. Lee, and Y. H. Lee, "Birefringence induced by irregular structure in photonic crystal fiber," Opt. Express **11**, 2799-2806 (Nov, 2003).
11. P. F. Mclsaac, "Symmetry-induced modal characteristics of uniform waveguides. I. Summary of results," IEEE Trans. Microwave Theory Tech. **MTT-23**, 421-429 (1975).
12. R. Guobin, W. Zhi, L. Shuqin, and J. Shuisheng, "Mode classification and degeneracy in photonic crystal fibers," Opt. Express **11**, 1310-1321 (2003).
13. J. C. Knight, T. A. Birks, and P. St. J. Russell, "Properties of photonic crystal fiber and the effective index model," J. Opt. Soc. Am. A **15**, 748-752 (2003).
14. M. W. Haakestad and H. E. Engan, "Acoustooptic properties of a weakly multimode solid core photonic crystal fiber," J. Lightwave Technol. **24**, 838-845 (2006).

#87353 - $15.00 USD Received 10 Sep 2007; revised 12 Oct 2007; accepted 12 Oct 2007; published 31 Oct 2007

1. Introduction

During the last decade, photonic crystal fibers (PCFs) have been extensively studied for various applications utilizing their unique capabilities such as endless single mode operation, tailored dispersion, high birefringence, and enhanced or suppressed optical nonlinearity [1-3]. These unique features come from the fact that optical properties of the guided modes in the core can be easily manipulated by changing the air-hole structure in the cladding. While significant attention has been paid to the study of core modes of PCFs, very little effort has been devoted to the study of cladding modes. The characteristics of the cladding modes play critical roles in devices that utilize the coupling between the core and the cladding modes [4, 5] as in the case of conventional fibers [6, 7]. In this paper, we describe systematic analysis of the mode field distributions along with their effective refractive indices for the cladding modes in a typical PCF structure. Calculations are performed by using the plane wave expansion method [8].

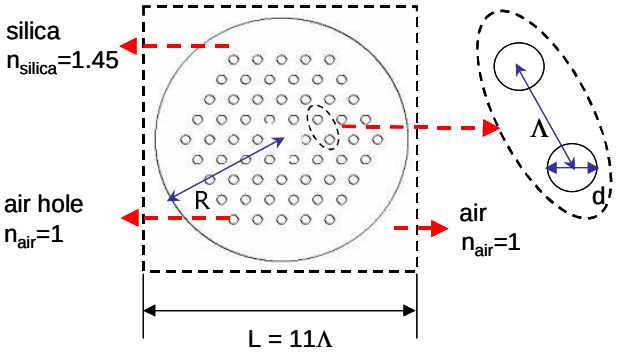

Fig. 1. The structure of PCF used in simulation. R: radius of PCF, Λ: distance between two adjacent holes, *d*: diameter of hole, L: supercell size.

The structure of the PCF analyzed in this work is shown in Fig. 1, which has four rows of air holes surrounding the silica core with a hexagonal symmetry. The cross-sectional structure consists of three main parts – a silica core, a holey cladding, and an outer silica region. The refractive indices used for silica and air are 1.45 and 1, respectively. For simplicity of calculation, we assume no material dispersion of silica. The pitch (Λ), the normalized air hole diameter (d/Λ), and the normalized outer diameters (2R/Λ) used for this calculation are Λ = 9.7 μm, d/Λ = 0.42, and 2R/Λ = 8.6 – 10.5 (2R = 83.5 - 102 μm), respectively. The PCF with these values was calculated to be a single-mode PCF where only the fundamental mode is guided in the core area. In Section 2, mode classification and degeneracy of the cladding modes are studied for the outer diameter of 83.5 μm. In Section 3, we calculate the mode indices and the field distributions for various outer diameters ranging from 83.5 to 102 μm in order to investigate the evolution of the cladding modes as a function of the outer diameter. In Section 4, we describe wavelength dependence of the mode indices, and also the modal beatlengths between the core and three lowest antisymmetric cladding modes in the PCF for the outer diameter of 84.5 μm.

2. Cladding modes of a PCF with a diameter of 83.5 μm

The plane wave expansion method uses the linear superposition of plane waves to build the electromagnetic field of the eigenmodes. For a given propagation constant (k), the optical frequency (ω), the complex amplitude of each plane wave component, and the mode field profile can be determined by using the electromagnetic variational theorem [9]. Our calculations were performed using a freely available software package [8]. The computational unit or the supercell is shown as a dashed rectangle in Fig. 1. Note that 2R = 83.5 μm is used

#87353 - $15.00 USD Received 10 Sep 2007; revised 12 Oct 2007; accepted 12 Oct 2007; published 31 Oct 2007

for the calculation in this section. The calculation accuracy is determined by several parameters such as the spatial resolution and the size of the supercell [10]. The spatial resolution represents the number of grids per pitch (Λ), and the total number of planewave bases used for the calculation is determined by $(L*\text{resolution})^2$. Due to the limited computation capacity of the PC used, we used the resolution of 48/Λ and the supercell size of 11Λ that produces the mode index error of $\sim 5\times10^{-5}$. In this case, we obtained a relative error in the index difference between two adjacent modes ($\sim 1\times10^{-7}$) that is small enough as a key parameter for devices utilizing core-cladding mode coupling.

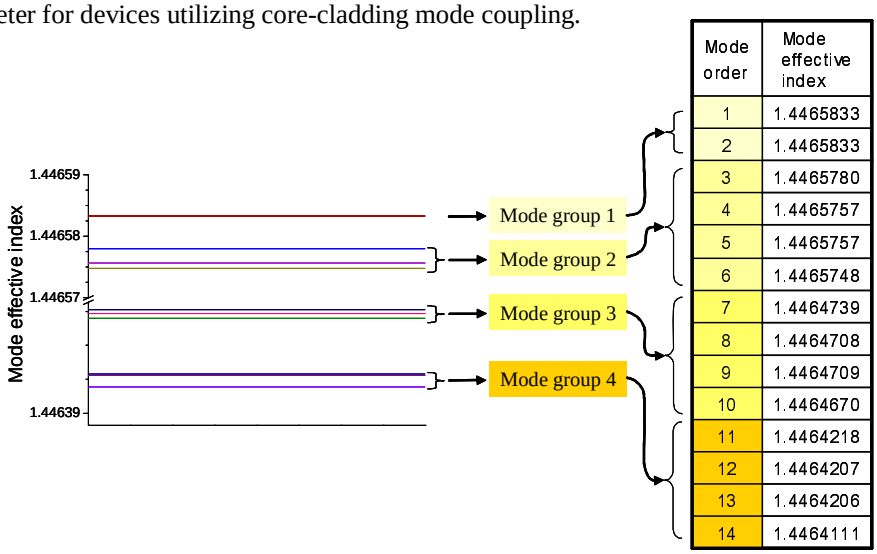

Mode order	Mode effective index
1	1.4465833
2	1.4465833
3	1.4465780
4	1.4465757
5	1.4465757
6	1.4465748
7	1.4464739
8	1.4464708
9	1.4464709
10	1.4464670
11	1.4464218
12	1.4464207
13	1.4464206
14	1.4464111

(a)

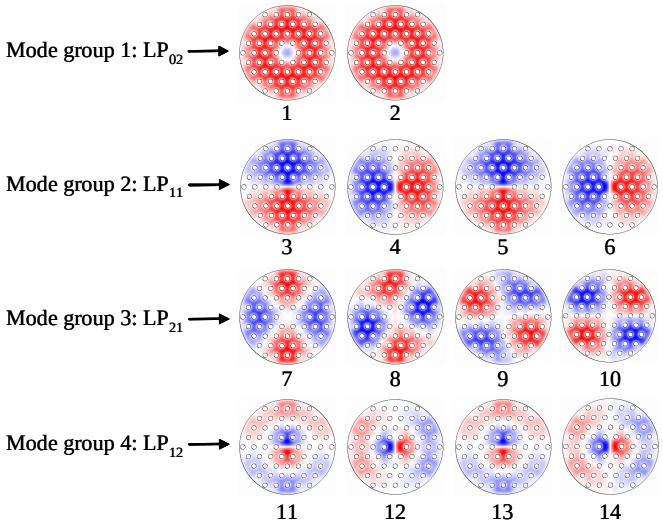

(b)

Fig. 2. (a). The mode effective indices and (b) the E_x field distributions of the lowest 14 cladding modes @ 2R=83.5 μm, λ=1.56 μm.

#87353 - $15.00 USD Received 10 Sep 2007; revised 12 Oct 2007; accepted 12 Oct 2007; published 31 Oct 2007

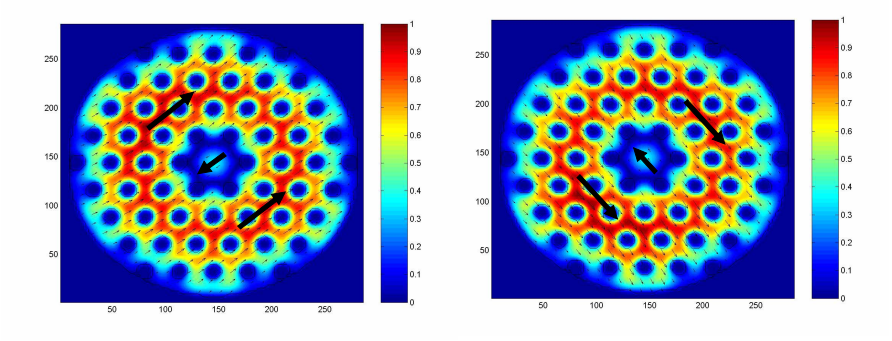

Fig. 3. The electrical field profiles of two degenerate modes of the first-order symmetric cladding mode @ 2R=83.5 μm, λ=1.56 μm.

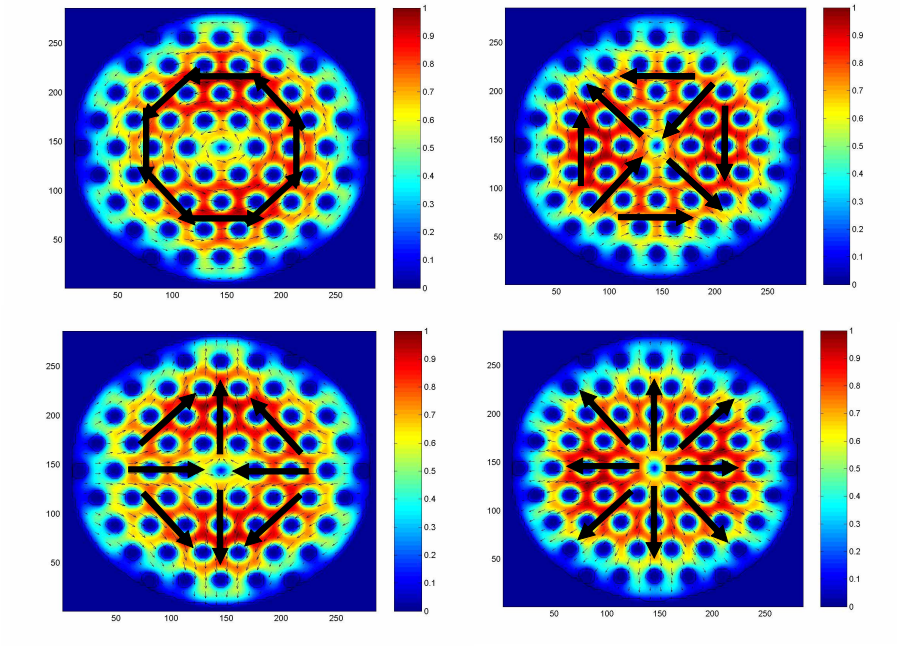

Fig. 4. The electrical field profiles of four degenerate modes of the first-order antisymmetric cladding mode @ 2R=83.5 μm, λ=1.56 μm.

Figure 2 shows the E_x field distributions and the mode effective indices of the lowest 14 cladding modes at the wavelength of 1.56 μm. As in the cases of conventional single-mode fibers, the nearly or completely degenerate modes can be grouped and labeled as LP_{nm} modes for the calculated cladding modes. It is interesting to note that the mode profiles in Fig. 2(b) are similar to their counterparts in conventional step-index circular fibers. Figure 3 shows the electrical field profiles of two eigen modes in the LP_{02} mode group with orthogonal polarization states (mode number 1 and 2 in Fig. 2). The mode index difference was calculated to be less than the calculation error (1×10^{-7}), and therefore, the two modes are considered degenerate. The two degenerate modes correspond to two HE_{12} modes in conventional step-index circular fibers. The LP_{11} mode group (mode number 3 ~ 6 in Fig. 2) has four nearly (not perfectly) degenerate modes of the TE_{01}, the HE_{21} even and odd, and the TM_{01} modes (see Fig. 4). The index difference between the HE_{21} even and odd modes is less

#87353 - $15.00 USD Received 10 Sep 2007; revised 12 Oct 2007; accepted 12 Oct 2007; published 31 Oct 2007

than the calculation error (1×10^{-7}), and those of TE_{01}-HE_{21} and HE_{21}-TM_{01} were calculated to be about 2.3×10^{-6} and 0.9×10^{-6}, respectively. The calculation results show that the degeneracy and also the field profiles of the mode group 1 (HE_{12}) and the mode group 2 ($TE_{01,}$ HE_{21} and TM_{01}) are equivalent to those of conventional step index fibers. This finding is consistent with predictions based on the group theory [11, 12], which states the fibers with circular and hexagonal cross-sections have the same mode classification. Exceptions are for the modes with the hexagonal symmetry in its field distribution such as HE_{3x} [12]. From the above considerations, we determined that the low order cladding modes can be approximated as linearly polarized (LP) modes as in the case of a conventional step-index fiber. In Section 3 and 4, the LP_{1x} modes in the PCF will be treated in detail since those are frequently used for core-cladding mode coupling devices.

3. Evolution of cladding modes as a function of diameter

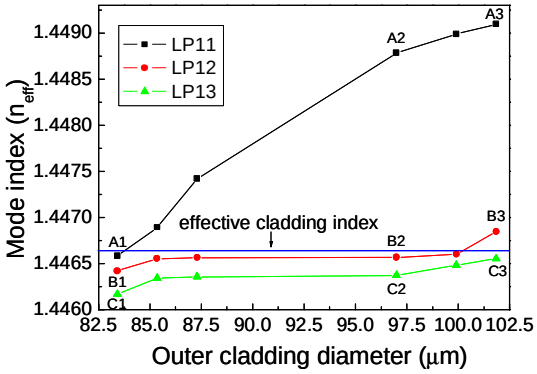

(a)

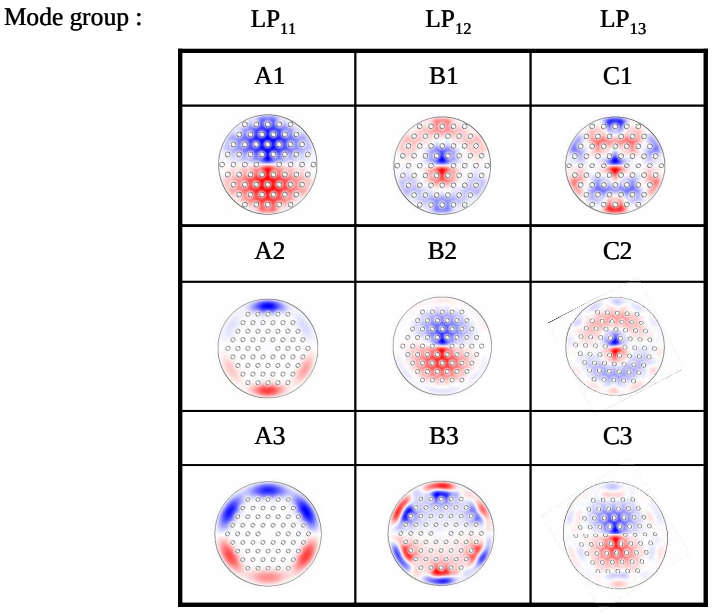

(b)

Fig. 5. (a). The mode indices and (b) the mode field profiles with x-polarization for the structure of PCF as a function of the outer diameter for antisymmetric modes @ λ=1.56 μm. Here, numbers 1, 2, and 3 denote three different values of the outer diameters (83.5, 97, and 102 μm, respectively).

#87353 - $15.00 USD Received 10 Sep 2007; revised 12 Oct 2007; accepted 12 Oct 2007; published 31 Oct 2007

Because a typical PCF has relatively large outer silica region surrounding an air-hole structure, it is important to understand its effects on the cladding mode properties. We examined the evolution of the cladding modes as a function of the outer cladding diameter. We repeated the calculation of the mode indices and the field distributions keeping the same area of the holey cladding structure while changing the outer diameter from 83.5 to 102 μm. Here, the upper limit of 102 μm was determined by the capacity of the personal computer used for calculations.

Figure 5 shows the E_x field distributions of three lowest-order LP_{1x} cladding modes at three different outer diameters and the mode indices as a function of the outer diameter at the wavelength of 1.56 μm. The horizontal straight line at 1.44667 in Fig. 5(a) denotes the magnitude of effective index of the cladding region with air holes, which represents the effective bulk material index of the infinitely periodic air-hole structure [13]. Interesting features are found in Fig. 5. As the diameter increases, the mode indices become higher and their field distributions shift into the outer ring region. Since cladding modes in a PCF are guided by the total internal reflection between the outer silica ring and the air around the fiber, higher mode indices and larger portion of the field distributions in the outer ring appear for cladding modes in a PCF with broader outer ring. The number of intensity nodes along the radial direction at each mode is maintained but their locations are shifted to the outer position along the radius. As the field intensity grows in the outer solid glass and decreases in the holey region, the mode indices become greater than the effective index of the holey cladding. Some modes in the figure (A2, A3, B3) have all the intensity nodes in the outer solid glass ring, and these 'ring modes' have already been referred as type 1 cladding modes in a recent publication [14]. It is also interesting to note that the modes A1-B2-C3 have similar field profiles except for the numbers of nodes in the outer ring region, and therefore similar effective indices.

4. Modal dispersion

In this section, we investigate dispersion properties of the cladding modes. Figure 6 shows (a) mode indices of the fundamental mode (LP_{01}) and the four LP_{1x} cladding modes and (b) the differences between the effective index of the holey structure and the four cladding mode indices, as a function of wavelength for the outer diameter of 84.5 μm. Here, the gray horizontal line in Fig. 6(b) is represents zero value which corresponds to the effective bulk index of the holey structure. Because of the strong dispersive property of the holey cladding, large dispersion slopes appear in all the cladding modes at longer wavelength. One can also see that index differences between two adjacent modes become bigger at the longer wavelength region in the Figs. 6(a) and (b).

Modal beatlengths between the fundamental core mode and the cladding modes are given by $L_B = \lambda/(n_{LP01} - n_{LP1x})$, and they are plotted as a function of wavelength in Fig. 6(c). The slopes of the beatlength curves are always negative, while they are positive in case of conventional single-mode fibers. It comes from highly dispersive property of the air-hole structure in the PCF. Guided modes in the PCF tend to have larger field distributions in the air holes at longer wavelengths; therefore, the magnitudes of mode effective indices become lower. In this case, the reduction of effective refractive index of the fundamental core mode at longer wavelengths due to the presence of the air holes is smaller than those for higher-order modes because the fundamental mode is most tightly confined in the silica core region. However, the magnitudes of the slopes in our PCF are similar to those of conventional fibers, and therefore we can expect similar coupling bandwidths of long period PCF gratings as in the case of conventional fiber counterparts. In the Fig. 6(c), we also indicated regions where the modes become the 'ring modes' described earlier, in contrast to the cladding modes that have the major optical power in the holey cladding region. One can see that the LP_{11} mode becomes a 'ring mode' at shorter wavelength region. It happens because the outer ring region can be regarded relatively thicker for a shorter wavelength. This transition point should be considered

#87353 - $15.00 USD Received 10 Sep 2007; revised 12 Oct 2007; accepted 12 Oct 2007; published 31 Oct 2007

seriously in mode coupling devices since the mode overlap between the core and the cladding modes will drop abruptly at a shorter wavelength than the transition point.

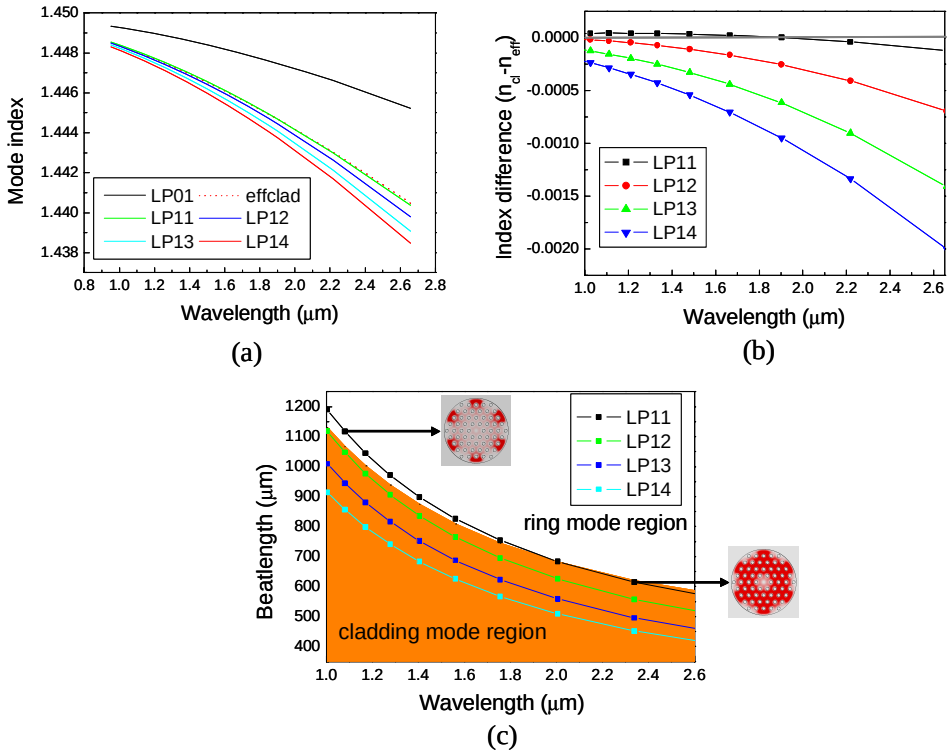

Fig. 6. (a). The refractive indices of the LP_{01} core mode and the four LP_{1x} cladding modes, (b) the relative index differences between the effective cladding and the four cladding modes, and (c) beatlengths between the core mode and the four cladding modes @ 2R=84.5 μm. Insets, the intensity distributions of the LP_{11} mode @ λ=1.08 and 2.34 μm.

5. Summary

We have calculated and analyzed the characteristics of the cladding modes in a standard PCF by using a plane wave expansion method. The classification of the cladding modes and their degeneracy were found to be similar to those of conventional step-index circular fibers. The dispersion properties of the cladding modes were also investigated and we found that it was mainly determined by that of holy cladding structure. This study provides essential information for design and development of cladding-mode-based applications of PCFs.

Acknowledgement

This work was supported by a grant from the Korea Research Foundation (R08-2004-000-10503-0).

#87353 - $15.00 USD Received 10 Sep 2007; revised 12 Oct 2007; accepted 12 Oct 2007; published 31 Oct 2007